Numerical simulations of intense charged-particle beam propagation in a dielectric wake-field accelerator

W. Gai,[1] A. D. Kanareykin,[2] A. L. Kustov,[2] and J. Simpson[1]
[1]*Argonne National Laboratory, 9700 South Cass Avenue, Argonne, Illinois 60439*
[2]*St. Petersburg Electrical Engineering University, 5 Professor Popov Street, St. Petersburg 197376, Russia*
(Received 24 July 1995; revised manuscript received 5 August 1996)

The propagation of an intense electron beam through a long dielectric tube is a critical issue for the successful demonstration of the dielectric wake-field acceleration scheme. Due to the head-tail beam breakup instability, a high-current beam cannot propagate long distances without external focusing. In this paper we examine the beam handling and control problem in the dielectric wake-field accelerator. We show that, by using an externally applied focusing and defocusing channel around the dielectric tube, a 150-MeV, 40-nC beam can be controlled and will propagate up to 5 m without significant particle losses for the proposed 15.6-GHz dielectric structures. We have also studied the case of a 100-nC beam propagating in a 20-GHz dielectric structure. Particle dynamics of the accelerated beam is also studied. Our results show that for typical dielectric wake-field accelerator structures, the head-tail instability of the accelerated beam can be conveniently controlled in the same way as the drive beam. [S1063-651X(97)02101-6]

PACS number(s): 41.60.Ap, 41.75.Lx, 41.85.Ja

I. INTRODUCTION

A different method of particle acceleration using wake fields (wake-field acceleration) excited by an intense electron beam passing through a slow-wave structure has been the subject of intensive studies as a promising technique to provide high gradients for electron acceleration. Dielectric-loaded waveguide structures provide particular advantages as a wake-field accelerator and have been the subject of both experimental and theoretical investigations in the past few years [1–3]. The principle of dielectric wake-field acceleration is to use the strong longitudinal wake field left behind by a short and intense driving beam to accelerate a less intense witness beam. One advantage of the dielectric wake-field accelerator is the simplicity of the structure. A proof of principle experiment has been successfully performed by Gai *et al.* [1].

The dielectric wake-field accelerator was initially proposed as a collinear wake-field scheme. According to the wake-field theorem [4], like all the other collinear wake-field schemes, the accelerated beam cannot gain more than twice the energy of the drive beam if the longitudinal shape of the drive beam is symmetric. Therefore, one needs a train of drive beams to accelerate the trailing beam to much higher energy than the drive beam. Each individual drive beam must be steered into different collinear wake-field structures. This procedure involves complicated beam manipulations and it is very difficult to achieve if the spacing of the drive bunches is very short. Another scheme to increase the total energy gain of the accelerated beam is to use multiple drive bunches traveling through a dielectric wake-field step-up transformer. The step-up transformer scheme is described in detail in Refs. [5,6] and the schematic diagram of the step-up transformer is shown in Fig. 1 The scheme is to extract rf power (longitudinal wake field) from the intense drive beam traveling in a relatively large diameter dielectric wake-field tube (stage I). This power is then transferred to a smaller diameter dielectric loaded guide (stage II) where the axial electric field is used to accelerate electrons. The key point of this step-up transformer scheme is that the dielectric constant in stage II is designed to be much higher than stage I, yielding a much lower group velocity. Field enhancement results both from the lower group velocity in stage II and from geometrical effects made possible by the use of dielectric loaded guides. When a large number of appropriately spaced electron drive pulses pass through stage I of the wake-field accelerator, a long rf pulse is produced, which is then fed into stage II. In this way, a high gradient and sustained long-distance acceleration can be obtained in stage II.

A strong longitudinal wake field also means that a strong transverse wake field can be generated if the drive beam in the structure is misaligned [7–9]. This deflection field can lead to severe head-tail single bunch beam breakup (BBU) instabilities of the drive beam. Beam breakup is the result of the transverse wake field of the leading particles in the beam deflecting the trailing particles. (In this paper BBU exclusively refers to the single-bunch head-tail instability.) If there are no corrections applied, a runaway effect will result in all the particles being lost by scraping on the inner wall of the structure. BBU in a conventional linear accelerator can be suppressed by introducing a momentum spread between the front and back of the beam and then propagating the beam through an alternating focusing channel [10], commonly known as Balakin-Novokhatsky-Smirnov (BNS) damping. Unlike a conventional linear accelerator, however, a wake-field accelerator uses a high charge and short drive beam. Because the wake fields are the result of coherent radiation from the drive beam, the tail portion of the beam loses energy much faster than the head portion. The momentum spread of the beam becomes very large. The quality of the rf produced in stage I is very sensitive to the change of the drive beam pulse length and particle loss. Severe particle loss in stage I will result in both rf phase and amplitude fluctuations.

Transport of a high-charge beam with large and changing momentum spread in the wake-field structure is critical to the

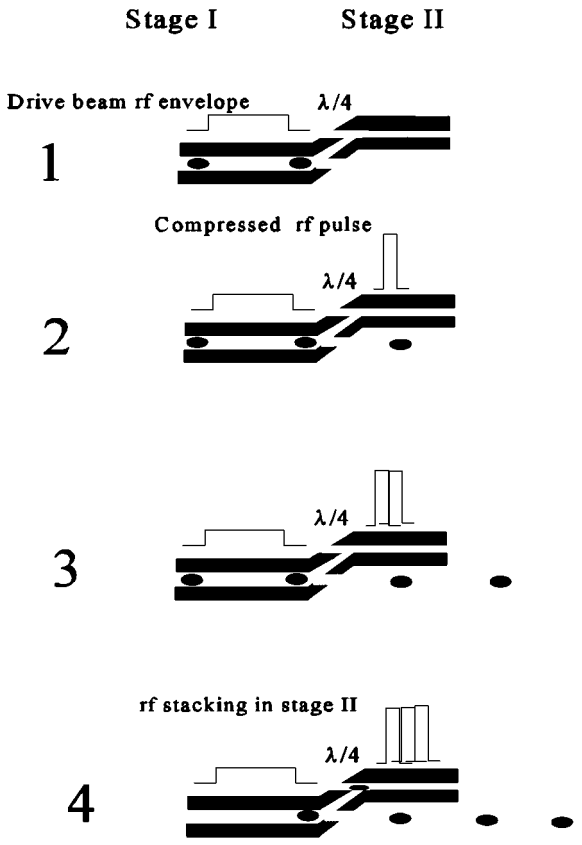

FIG. 1. Schematic diagram of multidrive beam step up transformer. The rf pulse generated in stage I is relatively long and low in amplitude. The pulse is fed into stage II, which will be used to accelerate a second charged-particle beam. The acceleration gradient in stage II is much higher than in stage I due to the *both* longitudinal (group velocity) and transverse (geometric) compression.

success of the wake-field acceleration concept. It determines the propagation distance of the beam, the efficiency of the device, and the quality of the wake field generated. Thus, controlling beam breakup effects in a wake-field accelerator is a very important issue and is the subject of this paper. We show that an alternating gradient focusing and defocusing channel (FODO) positioned around the dielectric wake-field tube through which the drive beam propagates can take advantage of the intrinsically large momentum spreads due to the longitudinal wakefield effect to produce an effect similar to the BNS damping. Due to the momentum spread in the beam, each particle oscillates at a different betatron frequency inside the alternating focusing channel. By appropriately adjusting the external focusing strength, the beam can be controlled [10].

We have developed a computer simulation code to simulate two-dimensional bunch dynamics (x,z) of the drive beam. We use the program to simulate the beam breakup effects in the proposed dielectric wake-field accelerator experiment at the Argonne Wakefield Accelerator (AWA).

Commissioning of the AWA is currently under way [11,13]. It is a facility that will generate (40–100)-nC, (15–20)-ps-long electron beams. It also produces a witness beam to probe the wake fields. A detailed description of the facility

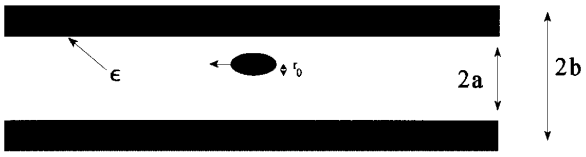

FIG. 2. Schematic of an electron beam passing through a dielectric wake-field tube. The tube is surrounded by conducting material. The transverse position of the beam is offset by x_0 from the tube center.

can be found in Ref. [13]. In phase I of the AWA project, the electron energy of the drive beam will be approximately 20 MeV. The design of phase II would increase the drive beam energy to 150 MeV. By using the step-up transformer scheme and the drive beam available during phase I of the AWA, we can accelerate a witness beam to over 100 MeV in 1 m or less. Experiments using both 40 and 100 nC drive beam energies are considered. The dielectric structure is chosen to have fundamental frequencies of 15.6 and 20 GHz. The drive beam is assumed to have dimensions of 1 mm (longitudinal) and 0.5 mm (transverse) rms and energies of 20 and 50 MeV.

II. WAKE FIELDS IN A DIELECTRIC STRUCTURE

Consider the dielectric structure as shown in Fig. 2. A charged particle traveling with velocity ν passing through the center of the structure with offset x_0 from the axis will leave behind both a longitudinal wake field W_z and transverse wake field W_x with frequency components ω_{mn} given by

$$W_z(z,x,t)=\sum_{m=0}^{\infty}\sum_{n=1}^{\infty}A_{mn}(s,a,b,\epsilon)I_m(kx_0)I_m(kx)\times\cos\left[\omega_{mn}\left(t-\frac{z}{\nu}\right)\right],$$

$$W_x(z,x,t)=\sum_{m=0}^{\infty}\sum_{n=1}^{\infty}B_{mn}(s,a,b,\epsilon)I_m(kx_0)I'_m(kx)\times\sin\left[\omega_{mn}\left(t-\frac{z}{\nu}\right)\right], \quad (1)$$

where $A_{mn}(s)$ and $B_{mn}(s)$ are functions of the geometric factors a,b,ϵ and the beam velocity $\beta=\nu/c$. The wake fields can be solved exactly as shown in Ref. [8] m and n are, respectively, the azimuthal and radial mode numbers of the wake fields in the dielectric wave guide. s and k are given by

$$s^2=\frac{\omega^2}{\nu^2}(\beta^2\epsilon-1), \quad k^2=\frac{\omega^2}{c^2}(1-\beta^2). \quad (2)$$

One would like to point out that for $m=0$, the transverse wake field goes to zero as the velocity of the electron ν approaches the speed of light c. Only higher-order azimuthal modes $(m\geqslant 1)$ have contributions to the transverse wake fields. Figure 3 shows the longitudinal wake field and Fig. 4 the transverse wake field excited by a 40-nC beam in a particular dielectric tube with $a=0.5$mm, $b=0.81$mm, and $\epsilon=3$.

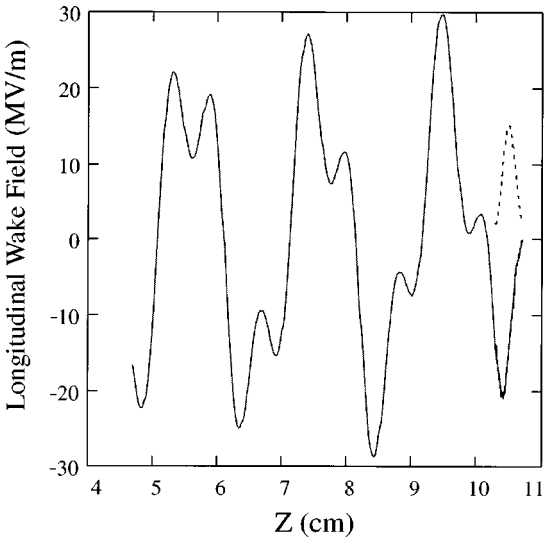

FIG. 3. Longitudinal wake field generated by a 40-nC beam with a rms bunch length of 1 mm in the dielectric wake-field structure with an inner radius of $a=5$ mm and outer radius $b=8.1$ mm. The solid line is the wake field and the dashed line is the drive beam.

III. BEAM DYNAMICS SIMULATIONS

A self-consistent computer code was developed to simulate the particle motion in the wake-field structures, which includes both longitudinal and transverse beam dynamics. The drive beam is assumed to have a two-dimensional Gaussian distribution, although other distributions can also be used. We assume that during a small time step of the calculation Δt both longitudinal and transverse wake fields remain constant. The time step was chosen small enough so that the results are not sensitive to the step size. The mode numbers used are $m=0, \quad n=1-4$ and $m=1, \quad n=1-3$. Higher-order modes have no significant contributions.

The drive beam is modeled by a distribution with total number of particles N. The ith particle at coordinates at z_i and x_i in the beam experiences the sum of both a longitudinal wake field W_z [Eq. (1)] and a transverse wake field W_x [Eq. (2)] generated by all the particles ahead of it. Causality is considered in summing over particles such that a given particle is affected only by those preceding it.

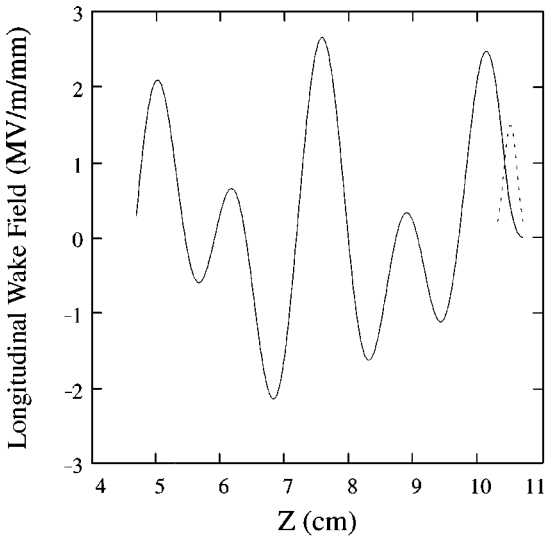

FIG. 4. Transverse wake field generated by the same beam in the same structure as in Fig. 3 with the beam offset $x_0=1$ mm.

The equation of motion of ith particle in the beam can be expressed as

$$\frac{dP_{z,i}}{dt}=W_z, \quad \frac{dP_{x,i}}{dt}+F(z,x)=W_{x,i}. \tag{3}$$

The external force $F(z)$ was chosen to be a periodic focusing force such as that produced by a FODO channel, which can be expressed simply as $F(z,x)=F(z)x$. The focusing force $F(z)$ is continuously applied around the tube to achieve the purpose of beam control. The strength of the focusing is tapered in the z direction to match the drive beam energy change. Every quadrupole has the same length. The focusing force $F(z)$ in the channel is assumed to vary as

$$F(z)=(-1)^{n+1}K_p\left(1-\eta\frac{z}{z_l}\right), \tag{4}$$

where n is the number representing the sequence number of the quadrupole. K_p is a constant that measures the strength of a quadrupole. Depending on whether the sequence starts from 0 or 1, it can be a focusing or defocusing element. $F(z)$ changes sign every 15 cm in all simulations. z_l is the total length of the wake-field device and η is the tapering factor. The alternating gradient focusing channel is applied continuously to the entire wake-field structure. Our program solves Eqs. (1c)–(4) simultaneously.

IV. PROPAGATION OF THE 40-NC BEAM IN THE DIELECTRIC STRUCTURES

In this section, we give the simulation results of the AWA beam propagating through the designed dielectric wake-field structures. We concentrate on the 40-nC case. The structure has an inner radius of 0.5 cm and outer radius of 0.81 cm with a dielectric constant of 3 giving a fundamental frequency of 15.6 GHz. The injected beam has energy of 20 or 150 MeV and an initial beam offset of 0.3 mm is used in both beam energies.

A. 20-MeV drive beam

First we consider the case of a 20-MeV drive beam (AWA phase I) and 40 nC charge with rms bunch length of 1 mm. The initial rms transverse dimension of the drive beam is 1 mm. The amplitude of the longitudinal wake field calculated here from Eq. (1) is 20 MV/m and the total length of the structure is 1 m.

1. Case I: No focusing applied

Figure 5 shows a sequence of a 40-nC drive bunch propagating through the dielectric tube with no external focusing applied. The horizontal axis is the distance traveled in the dielectric tube and the vertical is transverse position of the particles in the beam. Note that the limit of the vertical axis is from -5 to 5 mm, which represents the boundary of the dielectric tube. Due to the initial offset of the beam, the tail

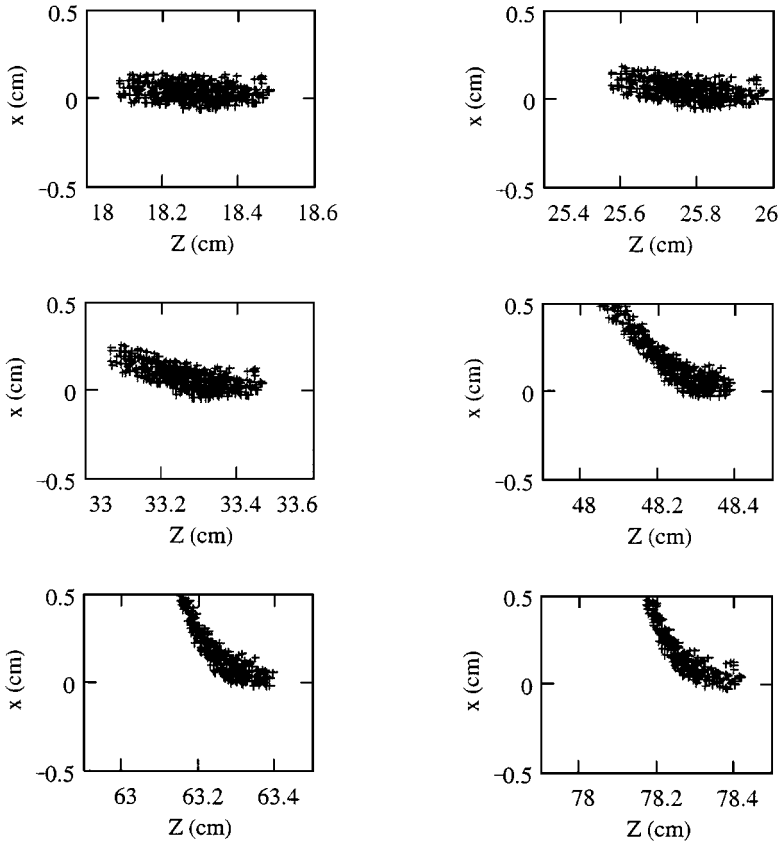

FIG. 5. 40-nC and 20-MeV beam traveling through a dielectric channel without any external focusing applied. Vertical (x) and horizontal axes (z) are transverse and longitudinal positions of a particle. Only a 0.3-mm initial beam offset will cause a loss of more than half the beam by 60 cm.

portion of the beam is deflected while it passes through the tube due to the transverse wake of the head. If a particle is deflected into the dielectric wall, the particle would be lost. The beam starts losing particles around 40 cm and more than half of the beam is lost by 60 cm. Therefore, even a small initial misalignment will cause severe beam loss.

2. Case II: Focusing applied

Next we consider the same case as above, except that an external focusing channel is applied around the dielectric tube. Focusing strength is adjusted to get the best results with $K_p = 1\ \mathrm{GV/m^2}$, where K_p is defined in Eq. (4). This corresponds to an initial betatron wavelength of $\lambda_\beta = 88.8\mathrm{cm}$. Due to the fact that the tail portion of the beam loses energy much faster than the front, each portion of the beam will have a different betatron wavelength. Therefore, each portion of the beam will oscillate incoherently around the axis of a structure. This is the fundamental mechanism for controlling BBU. The FODO lattice can be constructed by using a set of small permanent magnet quadrupoles. The tapering factor η of 0.5 is used here. The simulation result is shown in Fig. 6. The plots clearly show that the beam oscillates around the axis in a well-controlled manner. The front and tail of the beam oscillate at different frequencies, as expected. There is no significant particle loss before 80 cm. This is a significant improvement over the case of no focusing channel applied. After a 1.05 m path length, the driving beam has lost only 20% of its particles, the average energy is 12.09 MeV, and the energy spread has increased to 69%. The beam is dumped at this point because this method does not specify reacceleration of the drive beam.

B. 150-MeV, 40-nC beam in a dielectric structure with no external focusing

As discussed in the beginning of this section, phase II of the AWA project will provide a 150-MeV, (40–100)-nC drive pulse. Next we will simulate the beam transport in the same dielectric structures but over a much longer distance using this higher-energy beam.

As in Sec. IV A 1, the initial offset is also 0.3 mm. The simulation result is very similar to the 20-MeV drive beam case. The tail portion of the beam is deflected away gradually from the axis of the structures and into the dielectric wall, resulting in a severe beam loss. At a distance of 0.7 m the driving bunch has already lost 19% of its particles. The particle-loss process grows at a much faster rate as the bunches move further into the waveguide. After passing 1.5 m through the structure, the drive beam has lost most of its particles. At this point, almost all the beam reached the dielectric layer. Transverse focusing is therefore required for the long wake-field structure as described below. The simulation result is shown in Fig. 7.

C. 150-MeV, 40-nC beam in a dielectric structure with external focusing

We have studied carefully the case as above, but with external focusing applied as in the 20-MeV case. For $K_p = 12\ \mathrm{GV/m^2}$ and $\eta = 0.7$, as shown in Fig. 8, the beam can propagate to 4 m without any particle loss. The initial betatron wavelength is 70.2 cm. After 5.5 m, the particle loss only reached 20%.

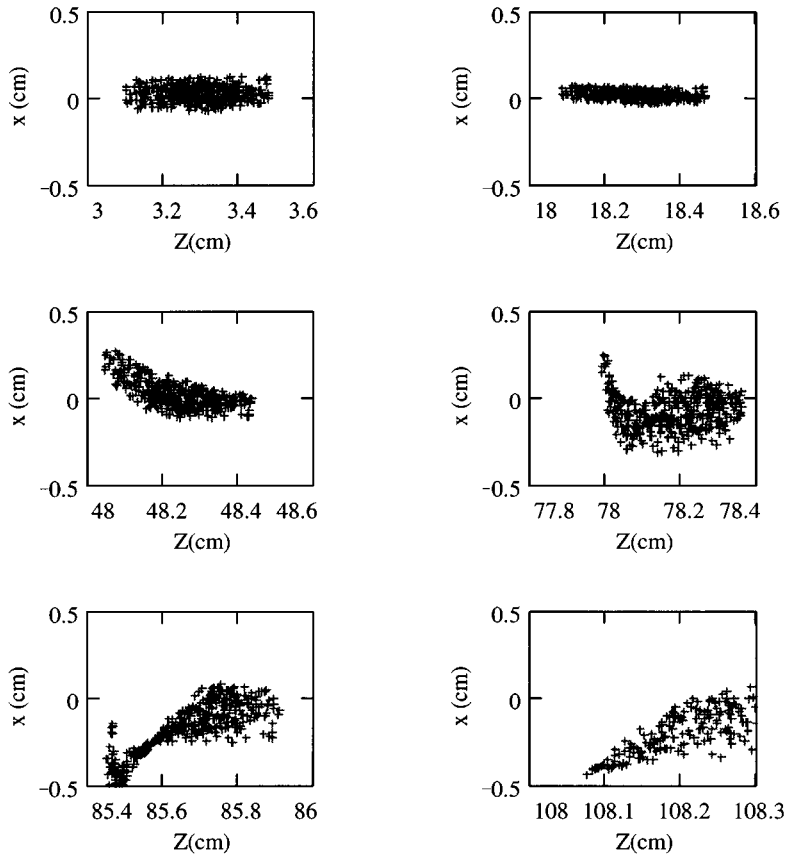

FIG. 6. Same case as in Fig. 3, except with external focusing applied. There is now no significant beam loss until it reaches more than 80 cm.

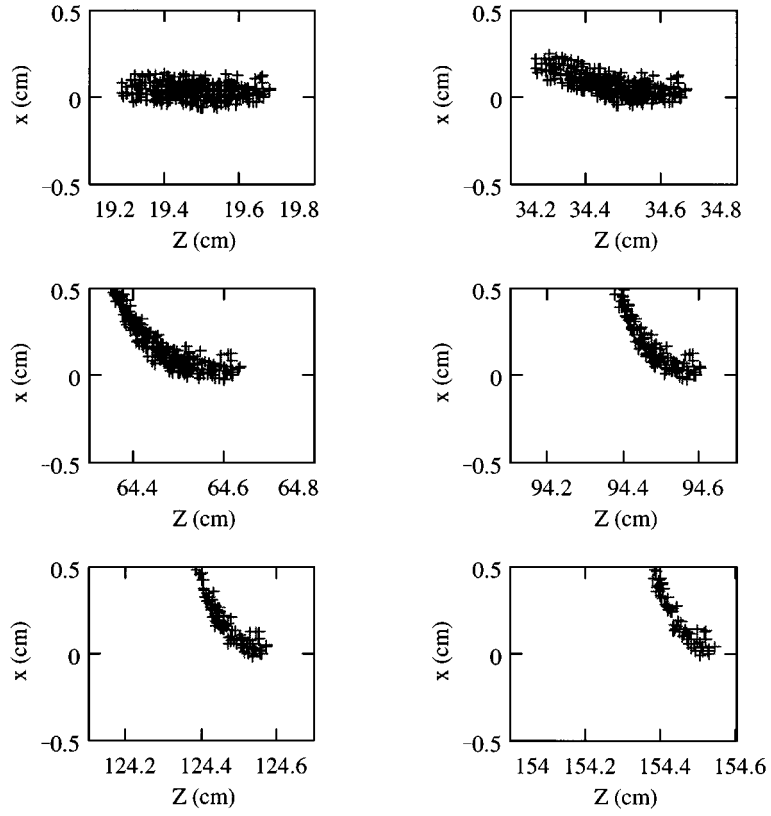

FIG. 7. 40-nC, 150-MeV beam propagating through the same structure as in Fig. 5, except with no external focusing applied. The beam starts losing particles at 50 cm and has lost 50% after 1 m. At 1.5 m, more than 75% of the particles were lost.

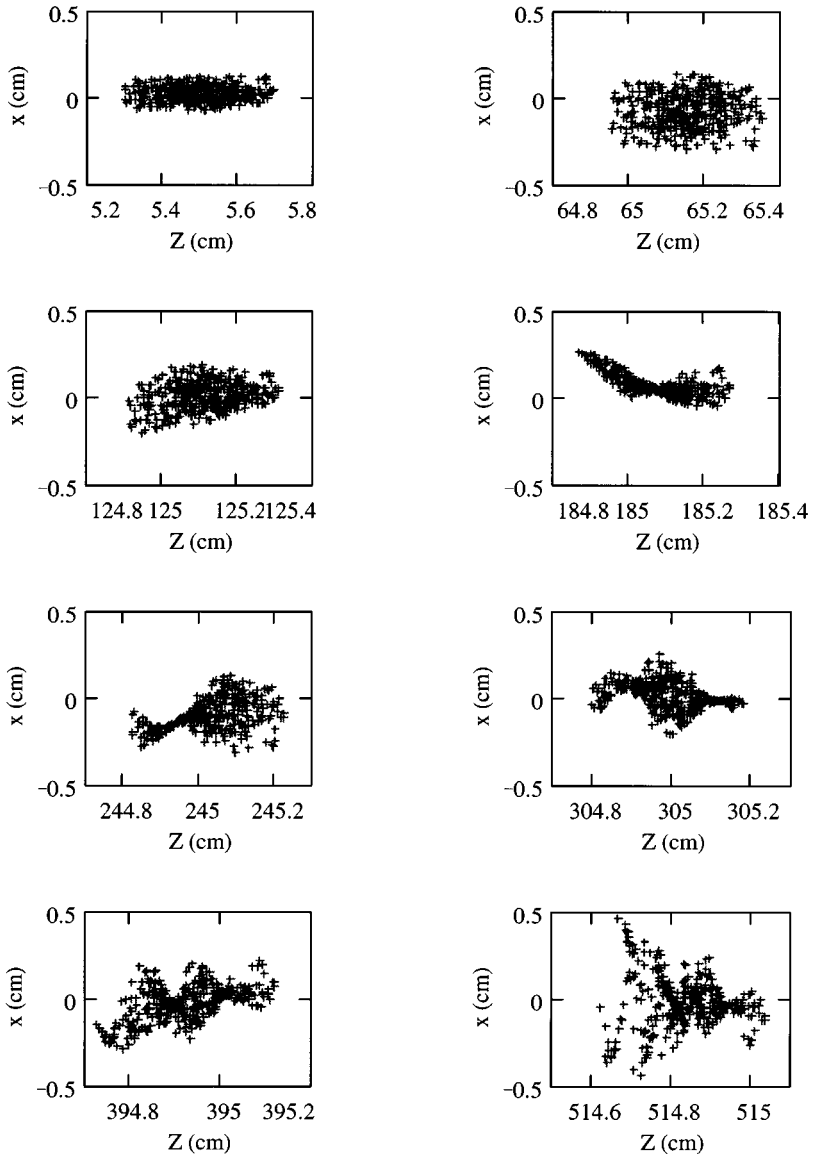

FIG. 8. Propagation of 40-nC beam in a 15.6-GHz structure with external focusing. The structure has 0.5 cm inner radius and 0.81 cm outer radius with a dielectric constant of 3. The beam propagates through more than 5.5 m without significant beam loss.

V. PROPAGATION OF A 100-NC BEAM IN DIELECTRIC STRUCTURES

We have also done the simulation of a 100-nC driving beam traveling through a 20-GHz dielectric structure with an outer radius of 0.91 cm, an inner radius of 0.75 cm, and a dielectric constant of 2.5. The peak longitudinal wake field is about 40 MV/m. A field step-up factor of 5 in the second stage would yield more than 200 MeV/m. As shown in Figs. 9 and 10, the beam has a very similar behavior to the previous cases. Without any external focusing, the beam cannot travel more than 2 m. However, a beam could propagate to 3 m without any significant particle losses with external focusing applied. The momentum spread of beam is 70% at this point. A similar simulation was also performed by K Ng [12]. He included quadrupole mode wake fields in his calculation and showed that the quadrupole wake fields play an important role in a thin-layer dielectric wake-field accelerator case when the beam needs to travel beyond 3 m. A larger initial offset of 0.6 mm is also considered here. For the same beam parameters as before, the results show that the beam still can travel 3 m without severe particle losses.

The cause of misalignment is very complicated. It can occur in both horizontal and vertical planes. For completeness, a situation where the first quadrupole is a defocusing element is considered. The result is worse than in the case where the first quadrupole is a focusing element. Although the initial offset is 0.3 mm in this case, the beam still can travel to 3 m. This is very understandable: a deflection in the first quadrupole is effectively the same as in the case of a larger initial beam offset. Our simulations verified this point.

VI. BEAM BREAKUP OF THE ACCLERATED BEAM

We have also investigated the beam breakup related effects for the accelerated beam (witness beam). The accelerated beam breakup problem in the step-up transformer scheme is the same as in conventional rf acceleration. Typically, the accelerated beam contains a relatively small amount of charge ($\sim$1 nC). Therefore, the head and tail beam breakup instability caused by the misalignment of the

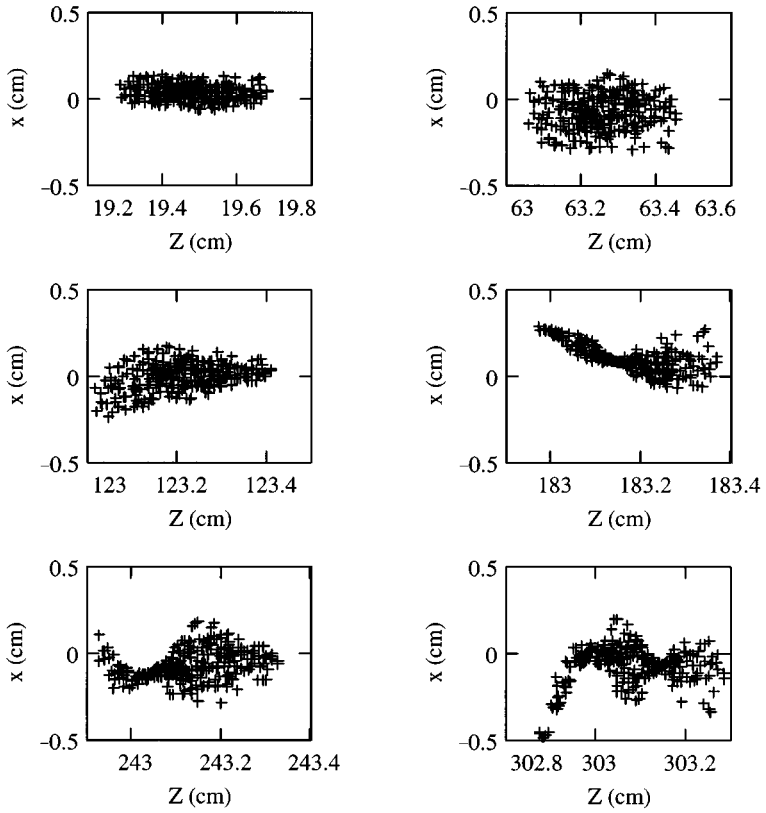

FIG. 9. 100-nC beam propagation through a 15.6-GHz structure. Less than 3% of the beam is lost after 3 m.

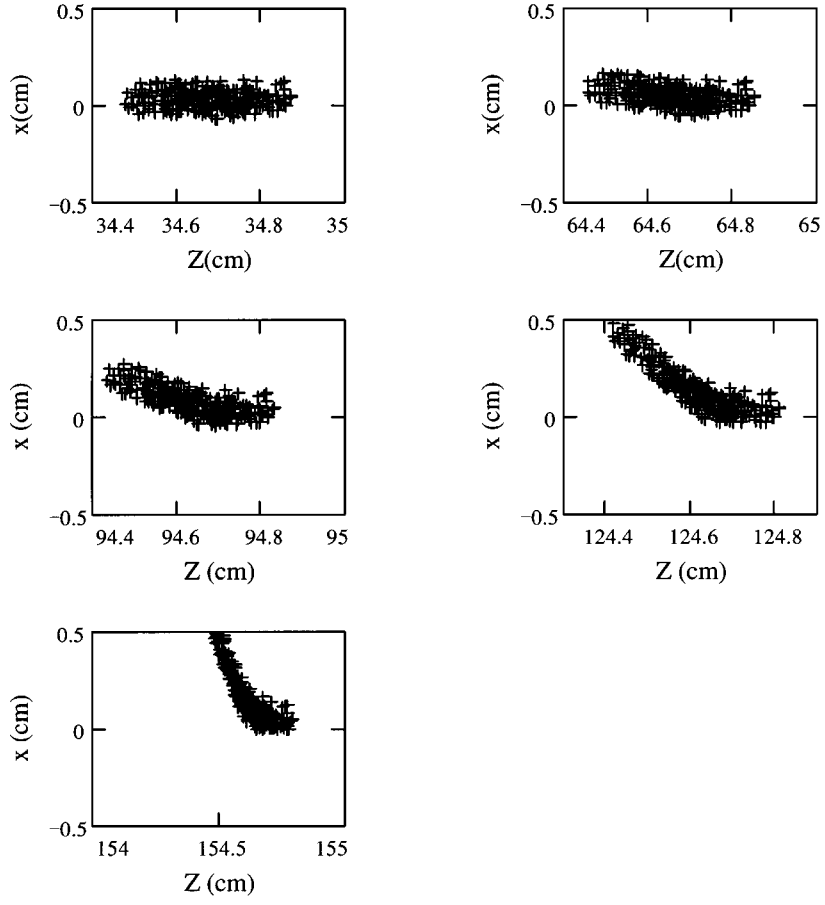

FIG. 10. Same as in Fig. 9, except no focusing is applied. The beam cannot propagate more than 1.5 m without losing half of its beam.

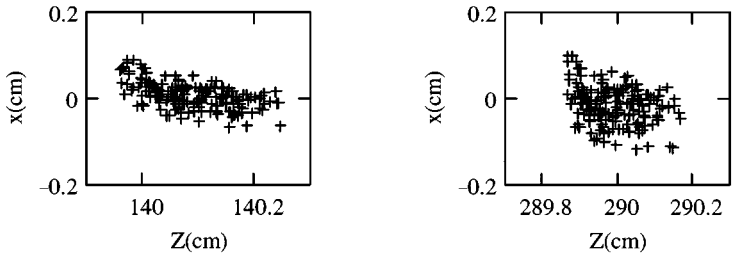

FIG. 11. Propagation of a 2-nC accelerated beam in stage II. The inner radius is 2 mm and the outer radius is 3.2 mm with a dielectric constant of 20. The fundamental rf of the structure is the same as in stage I: 15.6 GHz. The acceleration gradient is 100 MV/m and external focusing is also applied.

accelerated beam can be controlled in exactly the same way by using BNS damping.

In collinear acceleration, the witness beam is also affected by the misalignment of the drive beam. Similar to the drive beam case, our simulations show that an external focusing channel must be applied to control the witness beam. Because of the oscillations of the drive beam in the dielectric waveguide due to the external FODO channel, the net effect on the witness beam deflection is small.

Simulations for the accelerated beam dynamics have been performed for the same fundamental mode 15.4-GHz step-up transformer. We chose the parameters for stage II of the step-up transformer as inner radius of 2 mm and an outer radius of 3.2 mm with a dielectric constant of 20. Simulations were performed with an initial energy of 4 MeV and a total charge of 2 nC in the accelerated beam. An acceleration gradient of 100 MV/m was applied to simulate the long rf pulse extracted from stage I. The wake fields excited by the accelerated beam itself do not exceed 1 MV/m for the stage II parameters mentioned above. The effects of the head and tail beam breakup instabilities of the accelerated beam are much smaller when compared to the driving beam case. Figure 11 shows that particle losses were less than 3% after passing through a 3-m structure. The accelerated beam is completely controlled.

VII. SUMMARY

Successful propagation of intense charged beams in a dielectric wake-field structure is a critical issue for the viability of the dielectric wake-field concept. We have developed a computer program to simulate the beam propagation. The results are very encouraging. Our simulations show that by placing an alternating gradient magnetic focusing (FODO) channel around the dielectric tube, the beam breakup instability of the 40- and 100-nC beams with short bunch lengths can be controlled in a dielectric wake-field tube corresponding to the experiments planned at the Argonne Wakefield Accelerator. In the simulations all the quadrupole strengths need to be properly tapered to match the energy change of the drive beam. The same computer program is also used to simulate the beam breakup effect of the accelerated beam. It shows that in our present design, we can guide the whole accelerated beam as it passes through the accelerator without losses.

In summary, we have simulated the experimental parameters for dielectric device experiments planned for the Argonne Wakefield Accelerator. Our results show that the drive beam should be able to be transported through the dielectric structures and produce strong wake fields to achieve the goal of a 100 MV/m acceleration gradient.

ACKNOWLEDGMENTS

We appreciate the helpful discussions with P. Schoessow and his help on the simulation program developments. This work was supported by the U.S. Department of Energy, Division of High Energy Physics, Contract No. W-31-109-ENG-38.

[1] W. Gai, P. Schoessow, B. Cole, R. Konecny, J. Norem, J. Rosenzweig, and J. Simpson, Phys. Rev. Lett. **61**, 2756 (1988).
[2] Piwinski, DESY Report No. 72/72, 1972 (unpublished).
[3] R. Keinigs, M. Jones, and W. Gai, Part. Accel. **24**, 223 (1989).
[4] R. Ruth, A. Chao, P. Morton, and P. Wilson, Part. Accel. **17**, 171 (1985).
[5] E. Chojnacki, W. Gai, P. Schoessow, and J. Simpson, in *Proceedings of Particle Accelerator Conference*, edited by L. Lizama and J. Chew (IEEE, San Francisco, 1991), pp. 2557–2559.
[6] W. Gai and J. Simpson, *ANL-HEP-WF-173 (1993)* (unpublished).
[7] K. Y. Ng, Phys. Rev. D **42** 1819 (1990).
[8] M. Rosing and W. Gai, Phys. Rev. D **42** 1829 (1990).
[9] M. Jones, R. Keinigs, and W. Peter, Phys. Rev. A **46** 5183 (1992).
[10] K. Bane, AIP Conf. Proc. in *Physics of Particle Accelerators*, edited by Melvin Month and Margaret Deines, No. 153 (AIP, New York, 1987), p. 971.
[11] P. Schoessow *et al.*, in *Proceedings of Particle Accelerator Conference*, edited by S. Corneliussen (IEEE, Washington, D.C., 1993), pp. 2596–2598.
[12] K. Y. Ng, Int. J. Mod. Phys. A Proc. Suppl. **2** 511 (1993).
[13] P. Schoessow *et al.*, in *Proceedings of Particle Accelerator Conference*, edited by R. Sieman (IEEE, Dallas, 1995), pp. 976–978.